MARY KAY O'CONNOR PROCESS SAFETY CENTER
TEXAS A&M ENGINEERING EXPERIMENT STATION

19th Annual International Symposium
October 25-27, 2016 • College Station, Texas

# Analysis of enhanced flame speed in the transition droplet sizes for n-alkane aerosols generated by electrospray

*Yan-Ru Lin, Zhengdong Cheng and M. Sam Mannan**

Mary Kay O' Connor Process Safety Center, Artie McFerrin Department of Chemical Engineering, Texas A&M University, College Station, Texas 77843-3122, United States

*Corresponding Author: Tel.: +1 (979) 862-3985. Fax: +1 (979) 458-1493. E-mail: mannan@tamu.edu.

ABSTRACT

Fire and explosion incidents related to aerosol occur occasionally throughout the industries. However, its hazards are relatively overlooked due to the misconception of that liquids are safe below their flash point. As well as scarcity of data stems from the difficulty of aerosol generation by a well-controlled manner. In this research, n-alkane aerosols were produced from an improved electrospray device, and their flame speeds were measured to verify the transition range. When droplet sizes fell into this range, the flame speed would be enhanced and pose greater threats to people and surroundings. Theoretic simulation and empirical equation were performed to predict the trend of flame propagation. Application of convective droplet evaporation improved the theoretic simulation but still failed to recognize the transition range. On the other hand, the empirical equation provided a good fitting and explained possible reason for the trend. It should notice that the transition droplet size range is not a fixed range for aerosols. Therefore, process design and operation should consider the potential generation of aerosol size and location of transition range to reduce the hazards. By understanding the flammability of aerosol, the associated risk can be managed to an acceptable level.

**Keywords**: Flame speed, Transition range, Electrospray, Aerosol, Monodisperse

## 1. Introduction

Aerosol is suspension of minute particles in air. The droplets may be formed via condensation of vapor or mechanical breakup of liquid stream from high pressure orifice. In the process industry, there are numerous containers full of flammable or combustible materials stored at elevated

temperature and pressure. Once the materials release accidentally, they are capable of forming aerosol clouds and pose unexpected threats to personnel, plant and public. In 1974, Flixborough, UK, a large quantity of superheated cyclohexane flashed and condensed in the ambient condition. The aerosol cloud found an ignition source and the explosion demolished the plant, killing 28 personnel and injuring 36 others [1]. In 1995, there was a severe fire and explosion occurred in Milliken & Company's Live Oak/Milstar Complex and Carpet Service Center, causing the total loss of more than $400 million. The direct cause was leakage of hot oil with 350 $^{o}$F flash point. And the dense white cloud spread and reached an ignition source quickly [2].

It can be seen that a variety of hydrocarbons are capable of forming aerosol clouds and create huge losses, despite of low or high flash point. However, there is a misconception that liquids are quite safe when they are stored below their flash points, and standards often classify their hazardous degree by flash point [3, 4]. Unfortunately, those incidents have proven this is not proper [2, 5-7]. Therefore, more efforts and research should be conducted to resolve this issue.

Lower flammability limit (LFL) of aerosol has been studied widely, but no conclusive results can be determined. A general trend is observed that the lower flammability limit decreases as droplet size increases [8-11]. Burgoyne provided possible explanation that larger droplets possess higher settling speed, and the high settling speed creates higher local concentration, so called "kinetic" concentration [10]. Minimum ignition energy (MIE) is another aspect to consider flammability hazards. It is believed that the behavior of small droplets (*i.e.*, less than 10 μm) is same or similar to vapor form. Nevertheless, data and theoretical prediction of larger droplets are relative scarce as compared to vapor [12, 13].

Furthermore, the trend of aerosol flame propagation speed is not clear and even contradictory in literatures. Flame speed is the important factor to evaluate the hazardous consequences of materials. It is believed that the flame speed changes as droplet size shifts. However, there is no systematic approach to investigate aerosol flame speed and no definitive conclusion because of the difficulty of aerosol generation in a well-controlled manner. Some literatures show aerosol flame speed would only increase as droplet size decreases [14-18]. The maximum flame speed of such aerosols is flame speed of vapor, which can be achieved at very small droplet sizes, typically smaller than 10 μm. Interestingly, others demonstrate that there is a droplet size transition range. When droplet size is in this range, the associating aerosol flame speed would be even faster than that of smaller droplet sizes and vapor [19-23]. Moreover, some unclear patterns are also found [8, 24, 25]. All of these reveal there is contradictory observation regarding aerosol flame speed. If there is a transition range in which aerosol flame speed would be enhanced, then this range should be avoided to reduce the consequences if aerosol is likely to form. Therefore study on aerosol flame speed is necessary to prove the concept of transition range, both in experimental study and fundamental understanding.

In this research, three alkanes (n-octane, n-decane and n-dodecane) were atomized by using electrospray technique. The selection of fluids was based on their flash point, ranging from 286 K to 347 K. In order to increase their electric conductivity for electrospray application, 0.1 wt% of Stadis 450 was added into the hydrocarbons without changing other physical properties significantly [26]. The generated aerosols were further characterized to obtain their droplet sizes and associating flame speeds by Malvern laser diffraction particle analyzer and a high speed camera. Theoretical simulation was applied to explain the observed phenomenon.

## 2. Materials and methods

### *2.1. Materials*

In this study, three alkanes, n-octane, n-decane and n-dodecane, were being examined their aerosol flame propagation behavior by using electrospray device to produce aerosols. Their relevant properties are listed in Table 1. Since they are saturated hydrocarbons, their dipole moment and electric conductivity are too low to create aerosols by using electrospray technique. Therefore, an appropriate additive is necessary to promote their electric conductivity significantly without altering other properties obviously.

Several additives have been used in literatures, such as Stadis 450, Span 20, ionic liquids and alcohols. Stadis 450 was chosen because it demonstrated excellent ability to increase electric conductivity while other liquid properties remained consistent [26]. The amount of Stadis 450 was fixed at 0.1 wt% for all experiment. The liquid mixtures were stirred for 3 minutes and stood still over night to make sure they mixed homogeneously.

**Table 1**

Relevant properties of alkanes.

| | n-Octane | n-Decane | n-Dodecane |
|---|---|---|---|
| Molecular weight | 114.23 | 142.29 | 170.34 |
| Flash point (K) | 286 | 319 | 347 |
| Boiling point (K) | 399 | 447 | 489 |
| Density (kg/m$^3$) | 703 | 730 | 749 |
| Thermal conductivity (W/(m·K)) | 0.128 | 0.132 | 0.152 |
| Isobaric specific heat (J/(kg·K)) | 2228.8 | 2209.7 | 2207.4 |
| Heat of evaporation (J/kg) | 301147 | 272683 | 261242 |
| Heat of combustion (J/kg) | 47726096 | 47635111 | 47475637 |
| n[a] | 1.40 | 1.41 | 1.42 |
| k[a] | 0 | 0 | 0 |

[a] Refractive index is required for droplet size analysis. n and k are the real part and imaginary part of refractive index respectively.

### *2.2. Aerosol generation*

After samples were mixed well, they were aerosolized by a homemade electrospray system same as the previous study [4]. The samples were put into 10 syringes with 2.5 mL capacity. The syringes were pumped by a syringe propeller (KDS 220) and connected to plastic tubing (508 μm i.d.) and respective nozzles. The stainless steel nozzles (254 μm i.d. and 508 μm o.d.) were assembled on a compact disc and associated with a high voltage (HV1). A metal mesh connected to second high voltage (HV2) was aligned with the nozzles to create uniform electric field. The

voltage was generated by function generator (SRS, DS-345) and amplified to desired magnitude by amplifier (Trek Inc. 610E).

The stable operating parameters for aerosol generation had been discussed. Here the aerosols were generated within the stable range for consistent results. HV1 was set at 7 kV and HV2 was maintained at 5 kV (served as relative ground level). A flat grounded mesh (4 cm × 4 cm) and a cylindrical grounded mesh (4 cm in height and 10 cm in diameter) were positioned 15 cm beneath the HV2 metal mesh to collect the charged droplets. When liquid streams with suitable physical and electric properties go through the stainless steel nozzles, a conical shape of liquid stream can be observed and minute droplets are being produced from cone tip (cone-jet mode) [26, 27]. The schematic setup of electrospray device and overall system is displayed in Fig. 1.

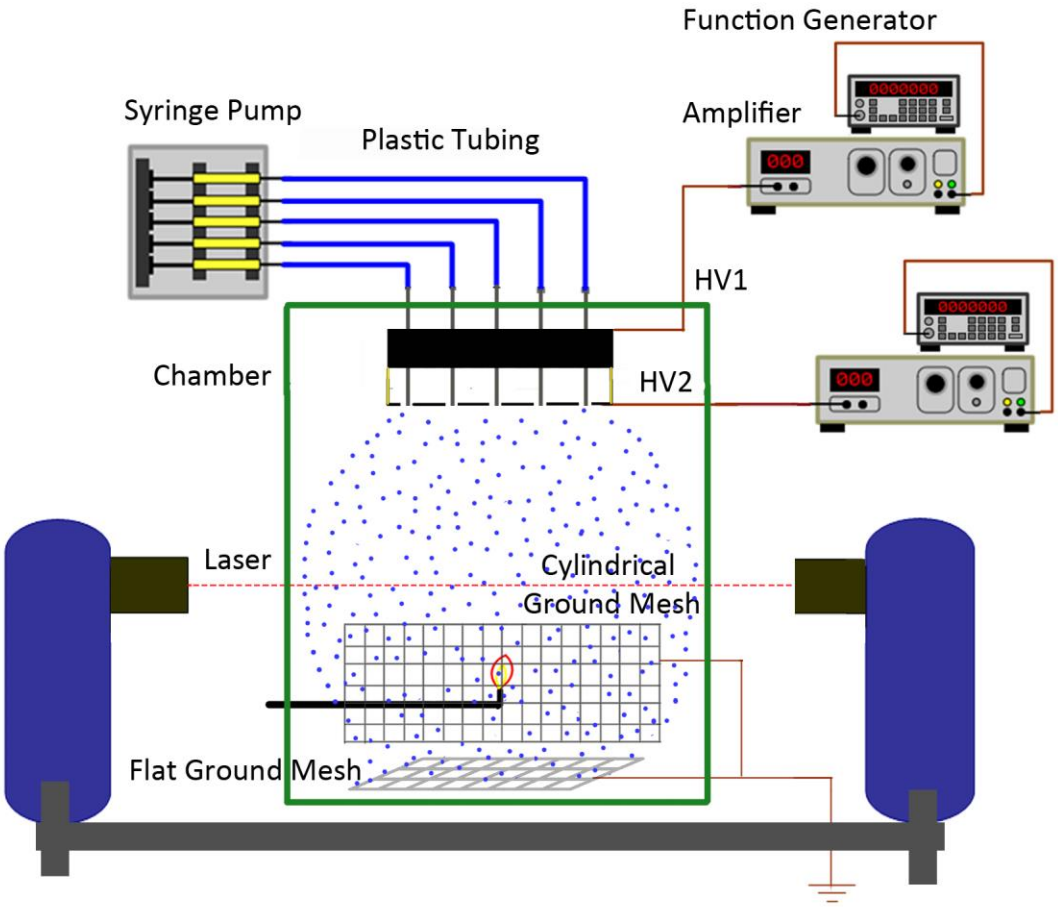


**Fig. 1. Schematic setup of electrospray device and overall system.**

*2.3. Aerosol characterization*

To monitor the aerosol cloud continuously without interrupting the generation process, a Laser Diffraction Particle Analyzer (SprayTec, Malvern Inc.) was used to obtain droplet size and aerosol

concentration [28]. The He-Ne laser has energy of 2 mW and is classified as 3R laser. All personnel in the lab should wear proper laser goggles while the laser is in operation.

The technique relies on Mie Theory and requires accurate refractive index ($n + ik$) to calculate the respective droplet size and concentration. The real part of refractive index provides information on how the light is scattered while the imaginary part describes the amount of laser energy being absorbed by droplets. The scattered angle of laser decreases logarithmically when droplet size increases. The droplet size reported here is based on Surface Area Moment Mean Diameter ($D_{32}$) or Sauter Mean Diameter (SMD). Aerosol concentration is further obtained by Beer-Lamber Law.

When aerosol cloud deemed stable, it was ignited by a 0.5 cm propane flame and the flame propagation was recorded by a high speed camera (Phantom 4.2, Vision Research Inc., the lens was DOZ-10x16 manufactured by Navitar) as described in literature [4]. The videos were further converted into a series of pictures with resolution of $512 \times 512$ pixels. The image analysis process was similar to Lian's method [29]. The presence of droplet created obstacles, and the relay propagation or inhomogeneous vapor distribution may result irregular flame propagation. Therefore, it was difficult to determine a flat flame front for flame speed calculation. Alternatively flame speed was calculated by moving center of flame bodies (*i.e.*, slope of flame position versus time).

*2.4. Flame speed model description*

Droplet evaporation plays an important role in aerosol flame propagation behavior and minimum ignition energy [13, 29]. If all droplets evaporate totally before encountering flame, then the behavior of this aerosol would be similar to vapor, which happens at very small droplets [30]. However, if droplets still present while contacting with flame, the droplets will absorb combustion heat and decelerate flame propagation. Other the other hand, the droplets can create turbulence and serve as obstacles to wrinkle flame front, which can increase surface reaction area and further enhance flame speed. To study the great complexity of droplet burning, a convective droplet evaporation model was utilized in energy and mass balance equations. The equations were further converted to relate to flame thickness and flame speed. Detailed model description and the necessary physical properties are as follows.

The convective droplet evaporation equation was given by Sirignano [31]:

$$\dot{m} = 2\pi \frac{kD_{32}}{C_p} \ln(1+B)\left(1 + \frac{cPr^{1/3}Re^{1/2}}{2F(B)}\right) \quad (1)$$

Where $\dot{m}$ is convective droplet vaporization rate (kg/s), $k$ and $C_p$ are thermal conductivity (W/(m·K)) and isobaric specific hear of gas (J/(kg·K)) respectively, $B$ is Spalding transfer number, c is a constant (0.848 from Ranz-Marshall's correlation), $Pr$ and $Re$ are Prandtl number and Reynolds number respectively, and $F(B)$ is a correlation of numerical results for Falkner-Marshall solutions.

The Spalding transfer number B or non-dimensional energy transfer number can be represented as eq. (2) according to Williams's work [32]:

$$\mathrm{B} = \frac{C_p(T_{ad}-T_b)+H_c Y_{O,\infty} f}{H_{vap}} \tag{2}$$

Where $T_{ad}$ and $T_b$ are adiabatic flame temperature (K) and boiling point (K) respectively, $H_c$ and $H_{vap}$ are heat of combustion (J/kg) and heat of vaporization (J/kg) of the liquid fuel respectively, $Y_{O,\infty}$ is oxygen concentration at the infinity distance, and $f$ is fuel to oxygen ratio.

Prandtl number and Reynolds number follow the eqs. (3) and (4) respectively.

$$\mathrm{Pr} = \frac{C_p \mu}{k} \tag{3}$$

$$\mathrm{Re} = \frac{\rho u_d D_{32}}{\mu} \tag{4}$$

Where $\mu$ and $\rho$ are gas dynamic viscosity (kg/(m·s)) and density (kg/m$^3$) respectively, and $u_d$ is droplet moving velocity (m/s).

Abramzon and Sirignano shows that the $\mathrm{F(B)}$ can be represented as [33]:

$$\mathrm{F(B)} = (1+\mathrm{B})^{0.7}\frac{\ln(1+\mathrm{B})}{\mathrm{B}} \qquad \text{for } 0 \le \mathrm{B} \le 20 \text{ and } 1 \le \mathrm{Pr} \le 3 \tag{5}$$

However, for $Re$ less than 10, eq. (1) should be corrected as

$$\dot{m} = 2\pi \frac{kD_{32}}{C_p} \ln(1+B)\left(1+\frac{c(1+2RePr)^{1/3}\max[1,(2Re)^{0.077}]-1}{2F(B)}\right) \tag{6}$$

Eqs. (2) to (6) provide how the droplet evaporation is influenced by liquid and gas properties and droplet moving velocity. The information needs to be further correlated with overall mass and energy balance to calculate laminar aerosol flame speed $S_{La}$ under steady state condition. According to Polymeropoulos's work [30], the energy balance relationship in the reaction zone can be associated with heat release from liquid fuel and vapor fuel combustion which equals to heat loss due to heat conduction to the surroundings as shown in eq. (7).

$$\dot{m}_t \Delta H t_q = \dot{m}_l \Delta H t_e + \dot{m}_v \Delta H t_c \tag{7}$$

Where $\dot{m}_t$, $\dot{m}_l$ and $\dot{m}_v$ are the total mixture mass flow rate (kg/s), the liquid phase flow rate at the instant of droplet ignition and the vapor phase flow rate at the instant of droplet ignition, respectively. The characteristic heat loss time $t_q$ and characteristic chemical reaction time for the vapor phase $t_c$ can be shown as eq. (8) and (9) based on Ballal and Lefebvre's study [14].

$$t_q = \frac{\alpha}{S_{La}^2} \tag{8}$$

$$t_c = \frac{\alpha}{S_{Lg}^2} \tag{9}$$

Where $\alpha$ is thermal diffusivity of gas ($m^2/s$), and $S_{Lg}$ is the laminar flame speed of gas mixture.

The characteristic droplet vaporization time $t_e$ at the instant of droplet ignition follows the relation:

$$t_e = \frac{mass\ of\ a\ droplet\ at\ ignition}{rate\ of\ evaporation} = \frac{\rho_l \times \frac{\pi}{6} \times D_i^3}{\dot{m}} \tag{10}$$

Where $\rho_l$ is liquid density, and $D_i$ is the droplet diameter at ignition. The $D_i$ can be calculated by considering ignition criterion for aerosol. However, Polymeropoulos showed that $D_i \cong D_{32}$ for isooctane aerosols when $D_{32} \geq 15\ \mu m$ approximately [30]. Therefore, $D_i \cong D_{32}$ was used in this work since the hydrocarbons tested in this research are more difficult to ignite.

Substitute eq. (6) into eq. (10) and obtain eq. (11).

$$t_e = \frac{\rho_l D_{32}^2}{12\alpha\rho \ln(1+B)\left(1+\frac{c(1+2RePr)^{1/3}\max[1,(2Re)^{0.077}]-1}{2F(B)}\right)} \tag{11}$$

The mass balance of the fuel from upstream to the point of ignition is

$$\dot{m}_t = \dot{m}_l + \dot{m}_v \Rightarrow \frac{\dot{m}_l}{\dot{m}_t} = 1 - \frac{\dot{m}_v}{\dot{m}_t} \tag{12}$$

And the mass fraction of this equation can be simplified by using upstream fuel fraction in vapor form, $\Omega$

$$\frac{\dot{m}_l}{\dot{m}} = (1-\Omega)\frac{D_i^3}{D_{32}^3} = (1-\Omega) \tag{13}$$

$$\frac{\dot{m}_v}{\dot{m}_t} = \Omega \tag{14}$$

The aerosol flame speed eq. (15) can be obtained by substituting eqs. (8), (9), (11), (13) and (14) into eq. (7)

$$S = \left\{\frac{(1-\Omega)\rho_l D_{32}^2}{12\alpha^2\rho \ln(1+B)\left(1+\frac{c(1+2RePr)^{\frac{1}{3}}\max[1,(2Re)^{0.077}]-1}{2F(B)}\right)} + \frac{\Omega}{{S_L}^2}\right\}^{-0.5} \tag{15}$$

## 3. Results and discussion

### *3.1. Experimental and simulation results of flame speed for n-octane aerosols*

The three hydrocarbons, n-octane, n-decane and n-dodecane, were examined by the instruments and experimental procedure outlined above. Due to the nature of electrospray and the difficulty of aerosol generation by a well-controlled manner, it is hard to target different droplet sizes with consistent concentration. As a result, the concentration of large droplet aerosol is usually slightly

higher than that of small droplet aerosol. However, the trend of flame propagation seems not to be changed by this variation.

In order to determine the adiabatic flame temperature, the equivalence ratio, ϕ, was taken as 0.7 after considering kinetic concentration [10]. The adiabatic flame temperature for these hydrocarbons was therefore set as 1880 K. The physical properties of gas mixtures were calculated at the temperature of $(T_{ad} + T_u)/3$ based on Polymeropoulos's work [30]. $T_u$ was upstream temperature or room temperature for this experiment (294 K).

The upstream fuel fraction in the vapor form, Ω, was taken as zero because the aerosols were produced from electrospray method instead of condensation. In addition, the saturated vapor pressure of these hydrocarbons is relatively low.

The laminar flame speed of these gas mixtures at the room temperature, $S_{Lg}$, was not found in the literature. In addition, the flash point of n-decane and n-dodecaen is higher than room temperature, which means their saturated vapor cannot be ignited at this condition. Therefore, their $S_{Lg}$ was calculated from elevated temperature. It is known that the flame speed of the same group hydrocarbons (*i.e.,* n-alkanes here) is similar, and $S_{Lg}$ has an exponentiation relationship with base $T$ and exponent $x$. A simple correlation eq. (16) can be obtained based on flame speed of n-octane at 353 K and that of n-decane at 403 K when the equivalence ratio was 0.7 [34]. As a result, $S_{Lg}(294\ K) = 0.21$ (m/s) was used throughout the simulation.

$$S_{Lg}(T_2) = S_{Lg}(T_1) \times (\frac{T_2}{T_1})^{2.14} \tag{16}$$

The experimental results and simulation prediction of flame speed for n-octane aerosols were shown in Fig. 2. The Reynolds number for the convective evaporation was calculated with $u_d = 3\ (m/s)$ according to Peng's work [29]. It can be observed that there was a transition range where the aerosol flame speed was enhanced (*i.e.,* the flame speed first increased with decreasing droplet size and reached a maximum. Then the flame speed reduced with further decreasing droplet size). This trend was also observed in literatures and there were models to predict the flame propagation. Polymeropoulos developed a model for isooctane aerosol and he used this model to fit Ballal and Lefebvre's work. Here the properties of n-octane were plugged into Polymeropoulos's model [30]. For droplets larger than 27 μm, the aerosol flame speed was underestimated. Moreover, the location of transition range was not predicted accurately. Zhu and Rogg also developed a model for n-octane aerosol [35]. The magnitude of flame speed was around the same level. But again, no transition range was predicted here. The current model provided a good fit when droplets were larger than 38 μm. However, it was unable to predict the transition range observed in the experiment.

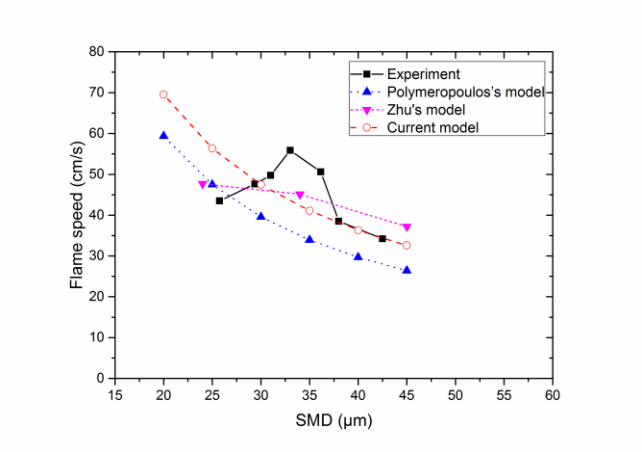


**Fig. 2. Flame speed of n-octane aerosols with experimental data, Polymeropoulos's model [30], Zhu's model [35] and current model.**

There are a few explanations why the enhanced flame speed would occur in the transition droplet size range. First, gases products released from burning droplets expanded hugely as compared to the small volume of liquid. This thermal expansion promotes mass and thermal transport, resulting higher reaction rate and flame speed. Second, the moving droplet has an elongated burning tail once it is ignited. The larger flame area may provide excess heat source for evaporation. In addition, droplet can be ignited in a different way as vapor does. Radiation heat may ignite a droplet without bringing the whole volume of gas/aerosol mixtures to the required temperature. There is another explanation for the relay propagation. If the flame radius of single droplet equals to the droplet spacing, the flame propagation would reach a maximum because the flame front contacts with droplet directly. Another possibility is that the vaporization of burning droplet provides the optimum range of fuel to oxygen ratio when certain droplet sizes and specific liquid properties are met. This can increase local combustion and thus promote overall flame speed. Finally, the presence of droplets serves as obstacles and wrinkles the flame front provided that the droplets are large enough and liquid volatility is adequate. The wrinkled flame has higher surface area for combustion and therefore flame speed is enhanced under the combination of droplet size and liquid properties. Photo evidence of wrinkled flame front of large droplets has been demonstrated in literature [19, 25]. It can also be observed that the flame front of smaller droplets is much smooth, which is similar to vapor form. These factors may intertwine together so a more robust model may be necessary to describe the complicated process.

In addition, sensitivity analysis was also conducted for $u_d = 1, 3\ and\ 6\ (m/s)$ as Deng's work demonstrated that droplet moving speed was around 6 m/s [36]. It can be seen that once convective droplet evaporation was considered in this model, the variation of aerosol flame speed was small as compared to Polymeropoulos's model (*i.e.*, not sensitive to droplet speed if it has been considered). However, current model cannot predict the location of enhanced flame speed although the magnitude of flame speed was close. It is possible that the moving droplet also has an impact on the ignition criterion. It should be considered to improve the model for transition range prediction in the future.

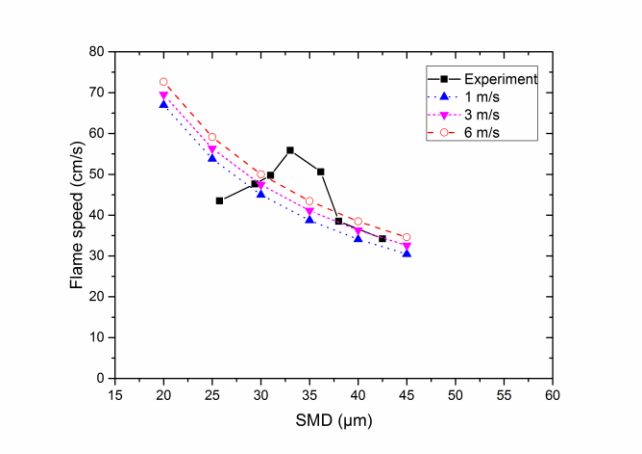


**Fig. 3. Sensitivity analysis of current model with droplet moving speed at 1, 3 and 6 m/s for n-octane aerosols.**

*3.2. Results of flame speed for n-decane and n-dodecane aerosols and the trend of transition droplet size range*

The results of aerosol flame speed for n-decane and n-dodecane were displayed in Fig. 4 and Fig. 5, respectively. Similarly, the phenomenon of enhanced flame speed was also observed for both n-alkanes. The transition droplet size cannot be predicted accurately. In addition, the model became less accurate when the number of carbon in the n-alkane increased. It was speculated that the vapor flame speed under room temperature ($S_{Lg}$) cannot be applied directly for n-decane and n-dodecane since the vapor from their liquid form is not flammable under this condition. Therefore, the deviation between experiment and simulation became larger as the carbon chain was longer.

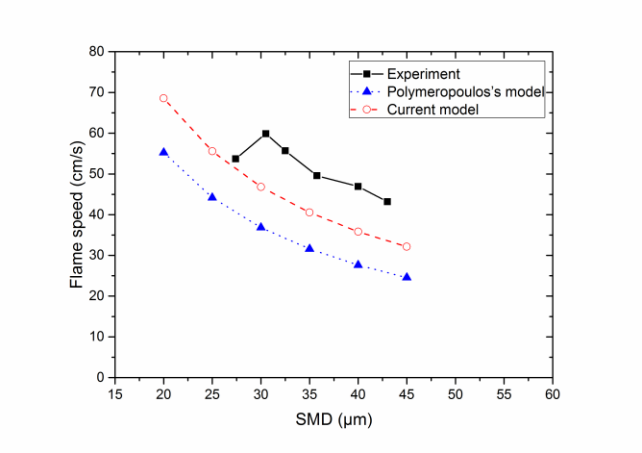


**Fig. 4. Flame speed of n-decane aerosols with experimental data, Polymeropoulos's model [30] and current model.**

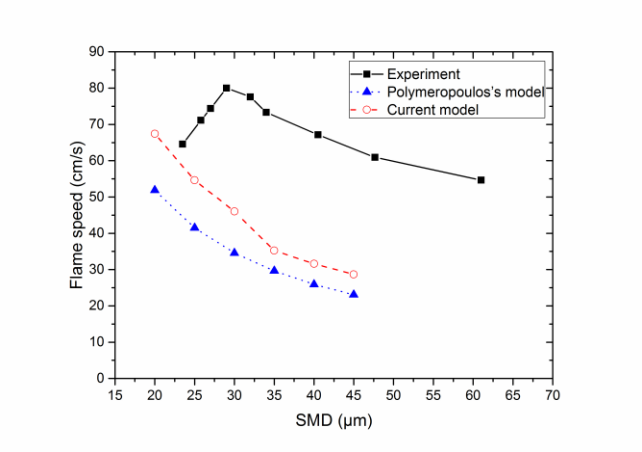


**Fig. 5. Flame speed of n-dodecane aerosols with experimental data, Polymeropoulos's model [30] and current model.**

Although the phenomenon of enhanced aerosol flame speed was seen on all three hydrocarbons here, the location of transition droplet size range may be not a fixed value. This behavior may change with liquid properties and concentration. The maximum flame speed was found when the aerosol diameter was between 10 and 20 μm for tetralin aerosols in Chan and Jou's test [20], which agreed with Polymeropoulos's prediction [30]. However, in Niioka's experiment [22], the maximum peak for n-decane aerosol was around 100 μm instead of 10 to 30 μm. Besides equipment and test differences, different volatilities/flash points and properties of the tested fuels may contribute to this discrepancy. The maximum peak of aerosol flame speed for n-octane, n-decane and n-dodecane in this study occurred around 33, 30.5 and 29 μm respectively, and their associating flash points are 286, 319 and 347 K.

It is reasonable to assume that the transition droplet size should be smaller for high flash point liquid (or lower volatility liquid) since it is not easy to evaporate or not easy to burn. So the transition size must be smaller to provide higher surface area for quick evaporation and subsequent combustion. On the other hand, for low flash point liquid (or higher volatility liquid), which is easy to evaporate or easy to burn, the transition size may be larger and still able to provide enough vapor for combustion.

There was a qualitative scheme for the selection of heat transfer fluids in the process industry. This selection mainly based on operating pressure and potential droplet size once leaked [37]. The smaller size the aerosol may be generated, the higher hazards the fluid may possess. However, it did not consider that the aerosol flame speed can be enhanced once the droplet size falls into the transition range. In addition, the location of transition range may not be a fixed value. Since flame speed of aerosol is higher than that of vapor under certain conditions, aerosol hazards may be more devastating than vapor form. In addition, people are relatively unaware of aerosol hazards. This clearly raises the need to investigate the flammability of aerosol and provide a thorough understanding. Then the preventative and mitigative measures can be made to avoid or reduce the associating risks.

## 4. Conclusions

The three n-alkane aerosols were produced by electrospray to examine their flame speed. It was found that the aerosol flame speeds for the three hydrocarbons were increased in a certain range of droplet sizes, so-called transition droplet size range. Model based on convective droplet evaporation, mass and energy balance was used to predict the trend of flame propagation. Although the magnitude of flame speed was acceptable for n-octane aerosols, the transition range was failed to recognize. Moreover, the deviation between experimental data and simulation became more obvious when the carbon chain got longer. This may due to the fact that the vapor flame speed under room temperature cannot be apply to the higher flash point of the liquids. Sensitivity of droplet moving speed was conducted. The results concluded that the effect of droplet speed was not significant once it had been considered in the model.

It is proved that the aerosol flame speed can be enhanced under certain conditions, which poses higher hazardous situation. Besides, the complexity of flame propagation and the paucity of flammability data all hinder the understanding of aerosol flammability. It is therefore necessary to research other fluids under the same or different conditions with regard to aerosol formation, flame speed, LFL and MIE. Then the use of such formation can help the selection of appropriate fluids and change of process parameters to make the process inherently safer. At least, when the potential of aerosol generation and transition range is identified, appropriate countermeasures must be employed to reduce the consequences/frequencies.

## Acknowledgments

This research was funded by the Mary Kay O' Connor Process Safety Center of the Chemical Engineering Department at Texas A&M University.

## References

[1] M.S. Mannan, Lee's loss prevention in the process industries. (3rd ed.), Elsevier, Burlington, MA, 2005.

[2] T.H. Miller, Live Oak/Milstar Complex and Carpet Service Center, in, United States Fire Administration, 1995.

[3] S.-y. Huang, X. Li, M.S. Mannan, The characterization of heat transfer fluid P-NF aerosol combustion: Ignitable region and flame development, Journal of Loss Prevention in the Process Industries, 26 (2013) 1134-1144.

[4] Y.-R. Lin, H. Chen, C. Mashuga, M.S. Mannan, Improved electrospray design for aerosol generation and flame propagation analysis, Journal of Loss Prevention in the Process Industries, 38 (2015) 148-155.

[5] H.L. Febo, J.V. Valiulis, Recognize the potential for heat-transfer-fluid mist explosions, Chem. Eng. Prog., 92 (1996) 52-55.

[6] HSE, Offshore hydrocarbon releases statistics and analysis, in, Bootle, Merseyside, UK, 2002.

[7] S.-y. Huang, X. Li, S. Mannan, Paratherm-NF aerosol combustion behavior simulation: ignition delay time, temperature distribution of flame propagation, and heat kernel hypothesis of combustion process analysis, Journal of Loss Prevention in the Process Industries, 26 (2013) 1415-1422.

[8] J.H. Burgoyne, L. Cohen, The effect of drop size on flame propagation in liquid aerosols, Proceedings of the Royal Society of London Series a-Mathematical and Physical Sciences, 225 (1954) 375-392.

[9] C.C. Miesse, Inhibition of flashing of aerosols, in, Armour Research Foundation of Illinois Institute of Technology, Arlington, VA, 1961.

[10] J.H. Burgoyne, The flammability of mists and sprays, in: Second Symposium of Chemical Process Hazards, 1963, pp. 1-5.

[11] S.J. Cook, C.F. Cullis, A.J. Good, The measurement of the flammability limits of mists, Combust. Flame, 30 (1977) 309-317.

[12] D.R. Ballal, A.H. Lefebvre, Ignition and flame quenching of flowing heterogeneous fuel-air mixtures, Combust. Flame, 35 (1979) 155-168.

[13] P. Lian, X. Gao, M.S. Mannan, Prediction of minimum ignition energy of aerosols using flame kernel modeling combined with flame front propagation theory, Journal of Loss Prevention in the Process Industries, 25 (2012) 103-113.

[14] D.R. Ballal, A.H. Lefebvre, Flame propagation in heterogeneous mixtures of fuel droplets, fuel vapor and air, Eighteenth Symposium (International) on Combustion, 18 (1981) 321–328.

[15] G.D. Myers, A.H. Lefebvre, Flame propagation in heterogeneous mixtures of fuel drops and air, Combust. Flame, 66 (1986) 193-210.

[16] J.B. Greenberg, I. Silverman, Y. Tambour, A new heterogeneous burning velocity formula for the propagation of a laminar flame front through a polydisperse spray of droplets, Combust. Flame, 104 (1996) 358-368.

[17] H. Nomura, K. Izawa, Y. Ujiie, J.i. Sato, Y. Marutani, M. Kono, H. Kawasaki, An experimental study on flame propagation in lean fuel droplet-vapor-air mixtures by using microgravity conditions, Symposium (International) on Combustion, 27 (1998) 2667-2674.

[18] X. Liu, Q. Zhang, Y. Wang, Influence of particle size on the explosion parameters in two-phase vapor–liquid n-hexane/air mixtures, Process Saf. Environ. Protect., 95 (2015) 184-194.

[19] S. Hayashi, S. Kumagai, T. Sakai, Propagation velocity and structure of flames in droplet-vapor-air mixtures, Combust. Sci. Technol., 15 (1977) 169-177.

[20] K.K. Chan, C.S. Jou, An experimental and theoretical investigation of the transition phenomenon in fuel spray deflagration: 1. The experiment, Fuel, 67 (1988) 1223-1227.

[21] Y. Nunome, S. Kato, K. Maruta, H. Kobayashi, T. Niioka, Flame propagation of n-decane spray in microgravity, Proc. Combust. Inst., 29 (2002) 2621-2626.

[22] T. Niioka, Flame propagation in sprays and particle clouds of less volatile fuels, Combust. Sci. Technol., 177 (2005) 1167-1182.

[23] N.N. Smirnov, V.N. Pushkin, V.R. Dushin, A.V. Kulchitskiy, Microgravity investigation of laminar flame propagation in monodisperse gas–droplet mixtures, Acta Astronautica, 61 (2007) 626-636.

[24] H. Nomura, M. Koyama, H. Miyamoto, Y. Ujiie, J.i. Sato, M. Kono, S.i. Yoda, Microgravity experiments of flame propagation in ethanol droplet-vapor-air mixture, Proc. Combust. Inst., 28 (2000) 999-1005.

[25] F. Atzler, F.X. Demoulin, M. Lawes, Y. Lee, N. Marquez, Burning rates and flame oscillations in globally homogeneous two-phase mixtures (flame speed oscillations in droplet cloud flames), Combust. Sci. Technol., 178 (2006) 2177-2198.

[26] K.Q. Tang, A. Gomez, Monodisperse electrosprays of low electric conductivity liquids in the cone-jet mode, J. Colloid Interface Sci., 184 (1996) 500-511.

[27] P. Lian, A.F. Mejia, Z.D. Cheng, M.S. Mannan, Flammability of heat transfer fluid aerosols produced by electrospray measured by laser diffraction analysis, Journal of Loss Prevention in the Process Industries, 23 (2010) 337-345.

[28] Malvern, Spraytec user manual, in, Worcestershire: Malvern Instruments Ltd., 2007.

[29] P. Lian, D. Ng, A.F. Mejia, Z.D. Cheng, M.S. Mannan, Study on flame characteristics in aerosols by industrial heat transfer fluids, Ind. Eng. Chem. Res., 50 (2011) 7644-7652.

[30] C.E. Polymeropoulos, Flame propagation in aerosols of fuel droplets, fuel vapor and air, Combust. Sci. Technol., 40 (1984) 217-232.

[31] W.A. Sirignano, Fluid Dynamics and Transport of Droplets and Sprays, Cambridge University Press, Cambridge, U.K., 2010.

[32] A. Williams, Combustion of Liquid Fuel Sprays, Butterworth & Co Ltd, London, UK, 1990.

[33] B. Abramzon, W.A. Sirignano, Droplet vaporization model for spray combustion calculations, International Journal of Heat and Mass Transfer, 32 (1989) 1605-1618.

[34] C. Ji, E. Dames, Y.L. Wang, H. Wang, F.N. Egolfopoulos, Propagation and extinction of premixed C5–C12 n-alkane flames, Combust. Flame, 157 (2010) 277-287.

[35] M. Zhu, B. Rogg, Modelling and simulation of sprays in laminar flames, Meccanica, 31 (1996) 177-193.

[36] W. Deng, A. Gomez, Influence of space charge on the scale-up of multiplexed electrosprays, J. Aerosol. Sci., 38 (2007) 1062-1078.

[37] K. Krishna, W.J. Rogers, M.S. Mannan, The use of aerosol formation, flammability, and explosion information for heat-transfer fluid selection, Journal of Hazardous Materials, 104 (2003) 215-226.